Pairing Correlations in Nuclear Systems, from Neutron Stars to Finite Nuclei

Morten Hjorth-Jensen*)

Department of Physics, University of Oslo, N-0316 Oslo, Norway

(Received January 15, 2002)

In this contribution we attempt at giving an overview of pairing correlations in nuclear systems with an emphasis on

- Superfluidity and superconductivity in neutron stars and the relation to the underlying nucleon-nucleon interaction.
- Extraction and interpretations of pairing correlations in finite nuclei through large-scale shell model studies of nuclei with mass $A \sim 100 - 132$. Effective interactions based on recent nucleon-nucleon interactions are utilized in the shell-model studies. The partial waves which lead to superfluid properties in infinite matter are also crucial for pairing correlations in finite nuclei.
- Discussion of recent experimental and theoretical studies of thermodynamical properties of finite nuclei and their interpretation in terms of eventual pairing transitions in finite nuclei.

§1. Introduction

Pairing correlations are expected to play an essential role in nuclear systems, ranging from the binding energy, excitation spectrum and odd-even effects in finite nuclei to superfluidity in the interior of neutron stars. A neutron star is perhaps the largest object in the universe which exhibits superfluidity in its interior. An eventual superfluid phase in a neutron star will condition the neutrino emission and thereby the cooling history of such a star, in addition to inducing mechanisms such as sudden spin ups in the rotational period of the star. For an infinite system, such as a neutron star, the nature of the pairing phase transition is well established as second order.

For finite nuclei there are several interesting manifestations of pairing correlations. In e.g., recent theoretical and experimental studies of thermodynamical properties of finite nuclei, the heat capacity has been found to exhibit a non-vanishing bump at temperatures proportional to half the pairing gap. These bumps have been interpreted as signs of the quenching of pair correlations, representing in turn features of the pairing transition for an infinitely large system. Furthermore, finite nuclei such as those found in the chain of even tin isotopes from ^{102}Sn to ^{130}Sn, exhibit a near constancy of the 2_1^+-0_1^+ excitation energy, a constancy which can be related to strong pairing correlations and the near degeneracy in energy of the relevant single particle orbits. Large shell-model calculations for these isotopes reveal that the major contribution to pairing correlations in the tin isotopes stems from the $^1S_0$ partial wave in the nucleon-nucleon interaction. Omitting this partial wave and the $^3P_2$ wave in the construction of an effective interaction, results in a spectrum

*) E-mail: morten.hjorth-jensen@fys.uio.no

which has essentially no correspondence with experiment. These partial waves are also of importance for infinite neutron matter and nuclear matter and give the largest contribution to the pairing interaction and energy gap in neutron star matter.

This contribution falls in four sections. After the above introductory words, we give a brief review of pairing in infinite neutron matter. Shell-model analyses of different approaches to the effective interaction are in turn made in §3. In the same section we discuss recent experimental and theoretical thermodynamical properties of finite nuclei. An interpretation in terms of eventual pairing transitions in finite nuclei is also presented. Concluding remarks are given in §4.

§2. Pairing in infinite neutron matter

The presence of neutron superfluidity in the crust and the inner part of neutron stars are considered well established in the physics of these compact stellar objects. In the low density outer part of a neutron star, the neutron superfluidity is expected mainly in the attractive $^1S_0$ channel. At higher density, the nuclei in the crust dissolve, and one expects a region consisting of a quantum liquid of neutrons and protons in beta equilibrium. The proton contaminant should be superfluid in the $^1S_0$ channel, while neutron superfluidity is expected to occur mainly in the coupled $^3P_2$-$^3F_2$ two-neutron channel. In the core of the star any superfluid phase should finally disappear.

The presence of two different superfluid regimes is suggested by the known trend of the nucleon-nucleon (NN) phase shifts in each scattering channel. In both the $^1S_0$ and $^3P_2$-$^3F_2$ channels the phase shifts indicate that the NN interaction is attractive. In particular for the $^1S_0$ channel, the occurrence of the well known virtual state in the neutron-neutron channel strongly suggests the possibility of a pairing condensate at low density, while for the $^3P_2$-$^3F_2$ channel the interaction becomes strongly attractive only at higher energy, which therefore suggests a possible pairing condensate in this channel at higher densities. In recent years the BCS gap equation has been solved with realistic interactions, and the results confirm these expectations.

The $^1S_0$ neutron superfluid is relevant for phenomena that can occur in the inner crust of neutron stars, like the formation of glitches, which may to be related to vortex pinning of the superfluid phase in the solid crust.[1)] The results of different groups are in close agreement on the $^1S_0$ pairing gap values and on its density dependence, which shows a peak value of about 3 MeV at a Fermi momentum close to $k_F \approx 0.8$ fm^{-1}.[2)−5)] All these calculations adopt the bare NN interaction or effective interactions without screening corrections as the pairing force. It has been pointed out that the screening by the medium of the interaction could strongly reduce the pairing strength in this channel.[5)−7)] However, the issue of the many-body calculation of the pairing effective interaction is a complex one and still far from a satisfactory solution.

The precise knowledge of the $^3P_2$-$^3F_2$ pairing gap is of paramount relevance for, e.g., the cooling of neutron stars, and different values correspond to drastically different scenarios for the cooling process. Generally, the gap suppresses the cooling by a factor $\sim \exp(-\Delta/T)$ (where Δ is the energy gap) which is severe for temperatures

Table I. Collection of $^3P_2$-$^3F_2$ energy gaps (in MeV) for the modern potentials discussed. BHF single-particle energies have been used. In case of no results, a vanishing gap was found.

k_F (fm^{-1})	CD-Bonn	V_{18}	Nijm I	Nijm II
1.2	0.04	0.04	0.04	0.04
1.4	0.10	0.10	0.10	0.10
1.6	0.18	0.17	0.18	0.18
1.8	0.25	0.23	0.26	0.26
2.0	0.29	0.22	0.34	0.36
2.2	0.29	0.16	0.40	0.47
2.4	0.27	0.07	0.46	0.67
2.6	0.21		0.47	0.99
2.8	0.17		0.49	1.74
3.0	0.11		0.43	3.14

well below the gap energy. Unfortunately, only few and partly contradictory calculations of the pairing gap exist in the literature, even at the level of the bare NN interaction.[8)−12)] However, when comparing the results, one should note that the NN interactions used in these calculations are not phase-shift equivalent, i.e., they do not predict exactly the same NN phase shifts. Furthermore, for the interactions used in Refs. 8)−11) the predicted phase shifts do not agree accurately with modern phase shift analyses, and the fit of the NN data has typically χ^2/datum ≈ 3. Progress has however been made not only in the accuracy and the consistency of the phase-shift analysis, but also in the fit of realistic NN interactions to these data. As a result, several new NN interactions have been constructed which fit the world data for *pp* and *np* scattering below 350 MeV with high precision. Potentials like the recent Argonne V_{18},[13)] the CD-Bonn[14)] or the new Nijmegen potentials[15)] yield a χ^2/datum of about 1 and may be called phase-shift equivalent. In Table I we show the recent non-relativistic pairing gaps for the $^3P_2$-$^3F_2$ partial waves, where effective nucleon masses from the lowest-order Brueckner-Hartree-Fock calculation have been employed, see Ref. 16) for more details. These results are for pure neutron matter and we observe that up to $k_F \sim 2$ fm^{-1}, the various potentials give more or less the same pairing gap. Above this Fermi momentum, which corresponds to a lab energy of ~ 350 MeV, the results start to differ. This is simply due to the fact that the potentials are basically fit to reproduce scattering data up to this lab energy. Beyond this energy, the potentials predict rather different phase shifts for the $^3P_2$-$^3F_2$ partial waves, see e.g., Ref. 16). Thus, before a precise calculation of $^3P_2$-$^3F_2$ energy gaps can be made, one needs NN interactions that fit the scattering data up to lab energies of ~ 1 GeV. This means in turn that the interaction models have to account for, due to the opening of inelasticities above 350 MeV, the $N\Delta$ channel.

The reader should however note that the above results are for pure neutron matter. We end therefore this section with a discussion of the pairing gap for β-stable matter of relevance for the neutron star cooling, see e.g., Ref. 17). We will also omit a discussion on neutron pairing gaps in the $^1S_0$ channel, since these appear at densities corresponding to the crust of the neutron star. The gap in the crustal material is unlikely to have any significant effect on cooling processes,[18)] though it is expected to be important in the explanation of glitch phenomena. Therefore,

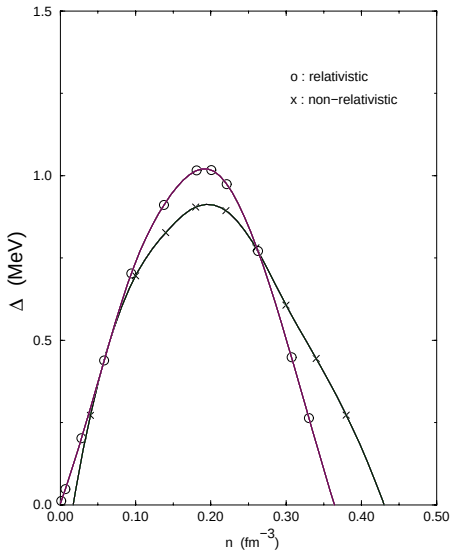

Fig. 1. Proton pairing in β-stable matter for the $^1S_0$ partial wave.

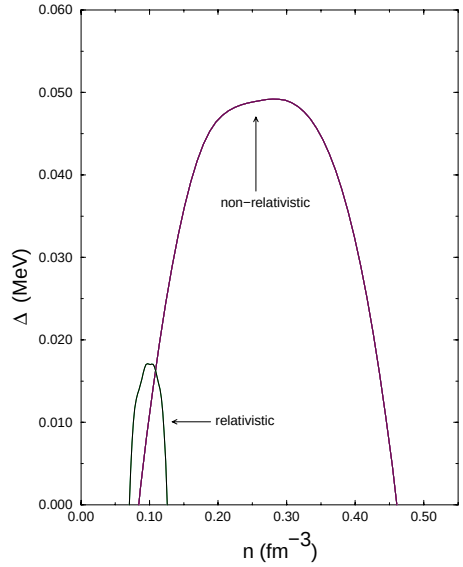

Fig. 2. Neutron pairing in β-stable matter for the $^3P_2$ partial wave.

the relevant pairing gaps for neutron star cooling should stem from the the proton contaminant in the $^1S_0$ channel, and superfluid neutrons yielding energy gaps in the coupled $^3P_2$-$^3F_2$ two-neutron channel. If in addition one studies closely the phase shifts for various higher partial waves of the NN interaction, one notices that at the densities which will correspond to the core of the star, any superfluid phase should eventually disappear. This is due to the fact that an attractive NN interaction is needed in order to obtain a positive energy gap. Since the relevant total baryonic densities for these types of pairing will be higher than the saturation density of nuclear matter, we will account for relativistic effects as well in the calculation of the pairing gaps. As an example, consider the evaluation of the proton $^1S_0$ pairing gap using a Dirac-Brueckner-Hartree-Fock approach. In Fig. 1 we plot as function of the total baryonic density the pairing gap for protons in the $^1S_0$ state, together with the results from the non-relativistic approach discussed in Refs. 11) and 19). These results are all for matter in β-equilibrium. In Fig. 1 we plot also the corresponding relativistic results for the neutron energy gap in the $^3P_2$ channel. For the $^3P_0$ and the $^1D_2$ channels we found both the non-relativistic and the relativistic energy gaps to vanish. As can be seen from Fig. 1, there are only small differences (except for higher densities) between the non-relativistic and relativistic proton gaps in the $^1S_0$ wave. This is expected since the proton fractions (and their respective Fermi momenta) are rather small. For neutrons however, the Fermi momenta are larger, and we would expect relativistic effects to be important. At Fermi momenta which correspond to the saturation point of nuclear matter, $k_F = 1.36$ fm^{-1}, the lowest relativistic correction to the kinetic energy per particle is of the order of 2 MeV. At densities higher than the saturation point, relativistic effects should be even more important. Since we are dealing with very small proton fractions, a Fermi momentum

of $k_F = 1.36$ fm^{-1}, would correspond to a total baryonic density ~ 0.09 fm^{-3}. Thus, at larger densities relativistic effects for neutrons should be important. This is also reflected in Fig. 2 for the pairing gap in the $^3P_2$ channel. The relativistic $^3P_2$ gap is less than half the corresponding non-relativistic one, and the density region is also much smaller, see Ref. 19) for further details. This discussion can be summarized as follows. The $^1S_0$ proton gap in β-stable matter is ≤ 1 MeV, and if polarization effects were taken into account,[5] it could be further reduced by a factor 2–3.

The $^3P_2$ gap is also small, of the order of ~ 0.1 MeV in β-stable matter. If relativistic effects are taken into account, it is almost vanishing. However, there is quite some uncertainty with the value for this pairing gap for densities above ~ 0.3 fm^{-3} due to the fact that the NN interactions are not fitted for the corresponding lab energies.

Higher partial waves give essentially vanishing pairing gaps in β-stable matter.

Thus, the $^1S_0$ and $^3P_2$ partial waves are crucial for our understanding of superfluidity in neutron star matter.

We have not mentioned recent developments beyond the BCS approach, nor have we discussed results for proton-neutron pairing in symmetric or asymmetric matter. Such topics are addressed in the recent works of Lombardo, Schulze and collaborators, see e.g., Refs. 20) and 21) and references therein.

§3. Pairing in finite nuclei

3.1. *Tin isotopes*

We turn the attention to finite nuclei. Here we focus on the chain of tin isotopes. Of interest in this study is the fact that the chain of even tin isotopes from ^{102}Sn to ^{130}Sn exhibits a near constancy of the $2_1^+ - 0_1^+$ excitation energy, a constancy which can be related to strong pairing correlations and the near degeneracy in energy of the relevant single particle orbits. As an example, we show the experimental*) 2_1^+-0_1^+ excitation energy from ^{116}Sn to ^{130}Sn in Table II. Our aim is to see whether the partial waves which played such a crucial role in neutron star matter, viz., $^1S_0$ and $^3P_2$, are equally important in reproducing the near constant spacing in the chain of even tin isotopes shown in Table II.

To achieve this, we mount a large-scale shell-model calculation in a model space relevant for the description of tin isotopes. In order to test the dependence on the above partial waves in the NN interaction, different effective interactions are employed.

Our scheme to obtain an effective two-body interaction for the tin isotopes starts with a free nucleon-nucleon interaction V which is appropriate for nuclear physics at low and intermediate energies. In this work we will thus choose to work with the charge-dependent version of the Bonn potential models, see Ref. 14). With this interaction, we compute effective two-particle matrix elements based on a $Z = 50$, $N = 82$ asymmetric core and with the active P-space for holes based on the $2s_{1/2}$,

*) We will limit our discussion to even nuclei from ^{116}Sn to ^{130}Sn, since a qualitatively similar picture is obtained from ^{102}Sn to ^{116}Sn.

Table II. 2_1^+-0_1^+ excitation energy for the even tin isotopes $^{130-116}$Sn for various approaches to the effective interaction. See text for further details. Energies are given in MeV.

	^{116}Sn	^{118}Sn	^{120}Sn	^{122}Sn	^{124}Sn	^{126}Sn	^{128}Sn	^{130}Sn
Expt	1.29	1.23	1.17	1.14	1.13	1.14	1.17	1.23
$V_{\rm eff}$	1.17	1.15	1.14	1.15	1.14	1.21	1.28	1.46
G-matrix	1.14	1.12	1.07	0.99	0.99	0.98	0.98	0.97
$^1S_0$ G-matrix	1.38	1.36	1.34	1.30	1.25	1.21	1.19	1.18

$1d_{5/2}$, $1d_{3/2}$, $0g_{7/2}$ and $0h_{11/2}$ hole orbits, see e.g., Refs. 22) and 23) for details. The corresponding single-hole energies are $\varepsilon(d^+_{3/2}) = 0.00$ MeV, $\varepsilon(h^-_{11/2}) = 0.242$ MeV, $\varepsilon(s^+_{1/2}) = 0.332$ MeV, $\varepsilon(d^+_{5/2}) = 1.655$ MeV and $\varepsilon(g^+_{7/2}) = 2.434$ MeV and the shell model calculation amounts to studying valence neutron holes outside this core. The shell model problem requires the solution of a real symmetric $n \times n$ matrix eigenvalue equation $\widetilde{H}\,|\Psi_k\rangle = E_k\,|\Psi_k\rangle$, where for the present cases the dimension of the P-space reaches $n \approx 2 \times 10^7$. At present our basic approach in finding solutions to shell-model problem is the Lanczos algorithm; an iterative method which gives the solution of the lowest eigenstates. This method was already applied to nuclear physics problems by Whitehead et al. in 1977. The technique is described in detail in Ref. 24), see also Ref. 25).

In order to test whether the $^1S_0$ and $^3P_2$ partial waves are equally important in reproducing the near constant spacing in the chain of even tin isotopes as they are for the superfluid properties of infinite matter, we study four different approximations to the shell-model effective interaction, viz.,

1. Our best approach to the effective interaction, $V_{\rm eff}$, contains all one-body and two-body diagrams through third order in the G-matrix, see Ref. 23).
2. The effective interaction is given by the G-matrix only and inludes all partial waves up to $l = 10$.
3. We define an effective interaction based on a G-matrix which now includes only the $^1S_0$ partial wave.
4. Finally, we use an effective interaction based on a G-matrix which does not contain the $^1S_0$ and $^3P_2$ partial waves, but all other waves up to $l = 10$.

In all four cases the same NN interaction is used, viz., the CD-Bonn interaction described in Ref. 14). Table II lists the results obtained for the three first cases.

We note from this table that the three first cases nearly produce a constant $2_1^+ - 0_1^+$ excitation energy, with our most optimal effective interaction $V_{\rm eff}$ being closest the experimental data. The bare G-matrix interaction, with no folded diagrams as well, results in a slightly more compressed spacing. This is mainly due to the omission of the core-polarization diagrams which typically render the $J = 0$ matrix elements more attractive. Such diagrams are included in $V_{\rm eff}$. Including only the $^1S_0$ partial wave in the construction of the G-matrix case 3, yields in turn a somewhat larger spacing. This can again be understood from the fact that a G-matrix constructed with this partial wave only does not receive contributions from any entirely repulsive partial wave. It should be noted that our optimal interaction, as demonstrated in Ref. 23), shows a rather good reproduction of the experimental spectra for both

Table III. 2_1^+-0_1^+ excitation energy for the even tin isotopes $^{130-124}$Sn obtained with a G-matrix effective interaction which excludes the important pairing waves $^1S_0$ and $^3P_2$. See text for further details. Energies are given in MeV.

	^{124}Sn	^{126}Sn	^{128}Sn	^{130}Sn
No $^1S_0$ and $^3P_2$ in G-matrix	0.15	−0.32	0.02	−0.21

even and odd nuclei. Although the approximations made in cases 2 and 3 produce an almost constant 2_1^+-0_1^+ excitation energy, they reproduce poorly the properties of odd nuclei and other excited states in the even Sn isotopes.

However, the fact that the first three approximations result in a such a good reproduction of the 2_1^+-0_1^+ spacing may hint to the fact that the $^1S_0$ partial wave is of paramount importance. If we now turn the attention to case 4, i.e., we omit the $^1S_0$ and $^3P_2$ partial waves in the construction of the G-matrix, the results presented in Table III exhibit a spectroscopic catastrophe. In this table we do also not list eigenstates with other quantum numbers. For e.g., ^{126}Sn the ground state is no longer a 0^+ state, rather it carries the quantum numbers 4^+ while for ^{124}Sn the ground state has 6^+. The first 0^+ state for this nucleus is given at an excitation energy of 0.1 MeV with respect to the 6^+ ground state. The general picture for other eigenstates is that of an extremely poor agreement with data. Since the agreement is so poor, even the qualitative reproduction of the 2_1^+-0_1^+ spacing, we defer from performing time-consuming shell-model calculations for ^{116,118,120,122}Sn.

3.2. *Thermodynamic properties of rare earth nuclei*

The thermodynamical properties of nuclei deviate from infinite systems. While the quenching of pairing in superconductors is well described as a function of temperature, the nucleus represents a finite many body system characterized by large fluctuations in the thermodynamic observables. A long-standing problem in experimental nuclear physics has been to observe the transition from strongly paired states, at around $T = 0$, to unpaired states at higher temperatures.

In nuclear theory, the pairing gap parameter Δ can be studied as function of temperature using the BCS gap equations.[26),27)] From this simple model the gap decreases monotonically to zero at a critical temperature of $T_c \sim 0.5\,\Delta$. However, if particle number is projected out,[28),29)] the decrease is significantly delayed. The predicted decrease of pair correlations takes place over several MeV of excitation energy.[29)] Recently,[30)] structures in the level densities in the 1–7 MeV region were reported, structures which probably are due to the breaking of nucleon pairs and a gradual decrease of pair correlations.

Experimental data on the quenching of pair correlations are important as a test for nuclear theories. Within finite temperature BCS and RPA models, level density and specific heat are calculated for e.g., ^{58}Ni;[32)] within the shell model Monte Carlo method (SMMC)[33),34)] one is now able to estimate level densities[35)] in heavy nuclei[36)] up to high excitation energies. Here we report on the observation of the gradual transition from strongly paired states to unpaired states in rare earth nuclei at low spin. The canonical heat capacity is used as a thermometer. Since only particles at the Fermi surface contribute to this quantity, it is very sensitive

to phase transitions. It has been demonstrated from SMMC calculations in the Fe region,[37)−39)] that breaking of only one nucleon pair increases the heat capacity significantly.

The experiments were carried out with 45 MeV ^{3}He projectiles from the MC-35 cyclotron at the University of Oslo. In that experiment, one could extract level densities and γ strength functions for the ^{161,162}Dy and ^{171,172}Yb nuclei. The data for the even nuclei are published recently.[30),31)]

The partition function in the canonical ensemble $Z(T) = \sum_{n=0}^{\infty} \rho(E_n) e^{-E_n/T}$ is determined by the measured level density of accessible states $\rho(E_n)$ in the present nuclear reaction. Strictly, the sum should run from zero to infinity. Here we calculate Z for temperatures up to $T = 1$ MeV. However, the experimental level densities only cover the excitation region up close to the neutron binding energy of about 6 and 8 MeV for odd and even mass nuclei, respectively. For higher energies it is reasonable to assume Fermi gas properties, since single particles are excited into the continuum region with high level density. Therefore, due to lack of experimental data, the level density is extrapolated to higher energies by the shifted Fermi gas model expression.[41)] The extraction of the microcanonical heat capacity $C_V(E)$ gives large fluctuations which are difficult to interpret.[30)] Therefore, the heat capacity $C_V(T)$ is calculated within the canonical ensemble, where T is a fixed input value in the theory, and a more appropriate parameter, see e.g., Schiller et al.[31)] for further details.

The deduced heat capacities for the ^{161,162}Dy nuclei are shown in Fig. 3 together with the SMMC results of Liu and Alhassid[39)] for various iron isotopes. The results

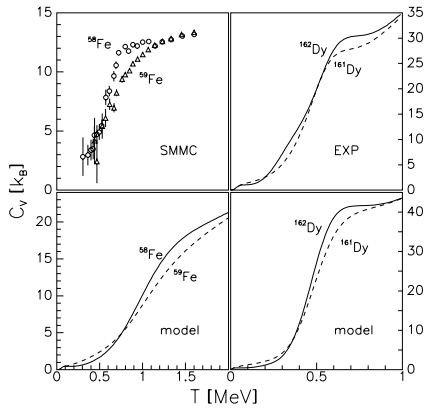

Fig. 3. Heat capacity for iron isotopes, see Ref. 39), and for ^{161,162}Dy. See text for further details.

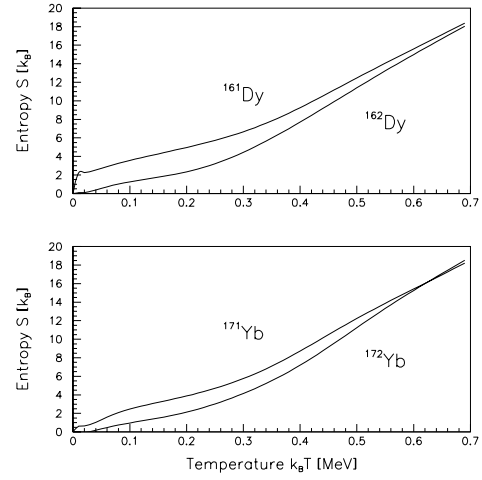

Fig. 4. Experimental entropy in the canonical ensemble for ^{161,162}Dy and for ^{171,172}Yb.

labelled 'model' are discussed further in Refs. 42) and 43). We note that both the theoretical and experimental results exhibit S-shaped $C_V(T)$-curves. The S-shaped curve is interpreted as a fingerprint of a phase transition in a finite system from a phase with strong pairing correlations to a phase without such correlations. Due to the strong smoothing introduced by the transformation to the canonical ensemble, we do not expect to see discrete transitions between the various quasiparticle regimes, but only the transition where all pairing correlations are quenched as a whole. It is worth noticing that the S-shape is much less pronounced for the odd system, again a possible indication of the importance of pairing correlations. This can also be seen from Fig. 4, taken from Ref. 44). Here we notice that the entropy of the even and odd systems merge at a temperature $T \approx 0.5$ MeV, in close agreement with the point where the S-shape of the heat capacity of the ^{161,162}Dy nuclei appears in Fig. 3. The temperature where the experimental entropies merge, could in turn be interpreted as the point where other degrees of freedom than pairing take over. A theoretical interpretation in terms of the vanishing of pairing correlations is given in Refs. 44) and 45).

§4. Conclusion

In summary, the $^1S_0$ and $^3P_2$ partial waves are crucial for our understanding of superfluidity in neutron star matter. In addition, viewing the results of Table III, one sees that pairing correlations, being important for the reproduction of the 2_1^+-0_1^+ excitation energy of the even Sn isotopes, depend strongly on the same partial waves of the NN interaction. Omitting these waves, especially the $^1S_0$ wave, results in a spectrum which has essentially no correspondence with experiment.

Furthermore, we have also discussed recent experimental and theoretical studies of thermodynamical properties of finite nuclei and their interpretation in terms of eventual pairing transitions in finite nuclei.

Acknowledgements

I am much indebted to Alexandar Belić (Belgrade), David Dean (ORNL), Torgeir Engeland (Oslo), Øystein Elgarøy (Cambridge), Magne Guttormsen (Oslo), Eivind Osnes (Oslo) and Andreas Schiller (LLNL) for the many discussion on the topics addressed here.

References

1) J. A. Sauls, in *Timing Neutron Stars*, ed. H. Ögelman and E. P. J. van den Heuvel (Dordrecht, Kluwer, 1989), p. 457.
2) M. Baldo, J. Cugnon, A. Lejeune and U. Lombardo, Nucl. Phys. A **515** (1990), 409.
3) V. A. Khodel, V. V. Khodel and J. W. Clark, Nucl. Phys. A **598** (1996), 390.
4) Ø. Elgarøy and M. Hjorth-Jensen, Phys. Rev. C **57** (1998), 1174.
5) H.-J. Schulze, J. Cugnon, A. Lejeune, M. Baldo and U. Lombardo, Phys. Lett. B **375** (1996), 1.
6) J. M. C. Chen, J. W. Clark, E. Krotschek and R. A. Smith, Nucl. Phys. A **451** (1986), 509.
J. M. C. Chen, J. W. Clark, R. D. Dave and V. V. Khodel, Nucl. Phys. A **555** (1993), 59.

7) T. L. Ainsworth, J. Wambach and D. Pines, Phys. Lett. B **222** (1989), 173.
J. Wambach, T. L. Ainsworth and D. Pines, Nucl. Phys. A **555** (1993), 128.
8) L. Amundsen and E. Østgaard, Nucl. Phys. A **437** (1985), 487.
9) M. Baldo, J. Cugnon, A. Lejeune and U. Lombardo, Nucl. Phys. A **536** (1992), 349.
10) T. Takatsuka and R. Tamagaki, Prog. Theor. Phys. Suppl. No. 112 (1993), 27.
11) Ø. Elgarøy, L. Engvik, M. Hjorth-Jensen and E. Osnes, Nucl. Phys. A **607** (1996), 425.
12) V. V. Khodel, PhD. Thesis, Washington University, St. Louis (1997).
V. A. Khodel, V. V. Khodel and J. W. Clark, Phys. Rev. Lett. **81** (1998), 3828; Nucl. Phys. A **679** (2001), 827; Phys. Rev. Lett. **81** (2001), 3828.
13) R. B. Wiringa, V. G. J. Stoks and R. Schiavilla, Phys. Rev. C **51** (1995), 38.
14) R. Machleidt, F. Sammarruca and Y. Song, Phys. Rev. C **53** (1996), 1483.
15) V. G. J. Stoks, R. A. M. Klomp, C. P. F. Terheggen and J. J. de Swart, Phys. Rev. C **49** (1994), 2950.
16) M. Baldo, Ø. Elgarøy, L. Engvik, M. Hjorth-Jensen and H.-J. Schulze, Phys. Rev. C **58** (1998), 1921.
17) H. Heiselberg and M. Hjorth-Jensen, Phys. Rep. **328** (2000), 237; nucl-th/9902033.
18) C. J. Pethick and D. G. Ravenhall, Ann. Rev. Nucl. Part. Sci. **45** (1995), 429.
19) Ø. Elgarøy, L. Engvik, M. Hjorth-Jensen and E. Osnes, Nucl. Phys. A **604** (1996), 466.
20) U. Lombardo and H.-J. Schulze, astro-ph/0012209, and references therein.
21) U. Lombardo, P. Nozieres, P. Schuck, H.-J. Schulze and A. Sedrakian, Phys. Rev. C **64** (2001), 064314.
22) M. Hjorth-Jensen, T. T. S. Kuo and E. Osnes, Phys. Rep. **261** (1995), 125.
23) A. Holt, T. Engeland, M. Hjorth-Jensen and E. Osnes, Nucl. Phys. A **634** (1998), 41.
24) R. R. Whitehead, A. Watt, B. J. Cole and I. Morrison, Adv. Nucl. Phys. **9** (1977), 123.
25) T. Engeland, M. Hjorth-Jensen, A. Holt and E. Osnes, Physica Scripta **T56** (1995), 58.
26) M. Sano and S. Yamasaki, Prog. Theor. Phys. **29** (1963), 397.
27) A. L. Goodman, Nucl. Phys. A **352** (1981), 45.
28) A. Faessler et al., Nucl. Phys. A **256** (1976), 106.
29) T. Døssing et al., Phys. Rev. Lett. **75** (1995), 1276.
30) E. Melby et al., Phys. Rev. Lett. **83** (1999), 3150.
31) A. Schiller et al., Phys. Rev. C **63** (2001), 021306(R).
32) Nguyen Dinh Dang, Z. Phys. A **335** (1990), 253.
33) G. H. Lang, C. W. Johnson, S. E. Koonin and W. E. Ormand, Phys. Rev. C **48** (1993), 1518.
34) S. E. Koonin, D. J. Dean and K. Langanke, Phys. Rep. **278** (1997), 1.
35) W. E. Ormand, Phys. Rev. C **56** (1997), R1678.
36) J. A. White, S. E. Koonin and D. J. Dean, Phys. Rev. C **61** (2000), 034303.
37) S. Rombouts, K. Heyde and N. Jachowicz, Phys. Rev. C **58** (1998), 3295.
38) Y. Alhassid, S. Liu and H. Nakada, Phys. Rev. Lett. **83** (1999), 4265.
39) S. Liu and Y. Alhassid, Phys. Rev. Lett. **87** (2001), 022501.
40) H. A. Bethe, Phys. Rev. **50** (1936), 332.
41) A. Gilbert and A. G. W. Cameron, Can. J. Phys. **43** (1965), 1446.
42) M. Guttormsen, M. Hjorth-Jensen, E. Melby, J. Rekstad, A. Schiller and S. Siem, Phys. Rev. C **63** (2001), 044301.
43) M. Guttormsen, M. Hjorth-Jensen, E. Melby, J. Rekstad, A. Schiller and S. Siem, Phys. Rev. C **64** (2001), 034319.
44) M. Guttormsen, A. Bjerve, M. Hjorth-Jensen, E. Melby, J. Rekstad, A. Schiller, S. Siem and A. Belić, Phys. Rev. C **62** (2000), 024306.
45) A. Belić, D. J. Dean and M. Hjorth-Jensen, cond-mat/0104138.